

Concrete Confinement Using Carbon Fiber Reinforced Polymer Grid

by A.P. Michael, H.R. Hamilton III, and M.H. Ansley

Synopsis: Corrosion of prestressing steel in precast concrete is a significant problem for coastal bridges in Florida. Replacement of prestressing steel with carbon fiber-reinforced polymer (CFRP) reinforcement provides a potential solution to this costly problem. The Florida Department of Transportation (FDOT) structures research center has teamed with the University of Florida (UF) to evaluate CFRP reinforced piles that employ two types of carbon reinforcement: (a) CFRP reinforcing bars and (b) CFRP grid. The CFRP bars act as flexural reinforcement while the CFRP grid provides confinement to the concrete core. The focus of this paper is on the confinement provided by the embedded CFRP grid, which is tied into a circular shape and cast into the concrete in a similar configuration to spiral ties. Existing confinement models are based on confinement provided by FRP wraps. Consequently, their use in predicting confinement must be validated with tests on embedded FRP grid. Standard (152 mm x 304 mm) concrete cylinders were cast both with and without the embedded CFRP grid. The cylinders were tested in compression to determine the effect of the CFRP grid on their strength and ductility. A significant improvement in ductility was observed for the cylinders with the embedded CFRP grid compared to the control cylinders.

Keywords: concrete; concrete strength; confinement; ductility; FRP materials; grid

992 Michael et al.

Antonis P. Michael is a graduate research assistant in the Department of Civil and Coastal Engineering at the University of Florida

H. R. Hamilton III is an associate professor in the Department of Civil and Coastal Engineering at the University of Florida

Marcus H. Ansley is the chief engineer at the Structures Research Center of the Florida Department of Transportation

INTRODUCTION

Corrosion of prestressing steel in precast concrete is a significant problem for coastal bridges in Florida. The use of carbon fiber-reinforced polymer (CFRP) composite reinforcement provides a potential solution to this costly problem. The Florida Department of Transportation (FDOT) structures research center has teamed with the University of Florida (UF) to evaluate the use of CFRP composite rebars as flexural reinforcement and CFRP composite grids as confinement to improve the concrete's strength and ductility in compression.

Column wrapping with CFRP composites is a popular alternative for improving the seismic resistance of columns. Fiber fabrics and prefabricated FRP composite jackets or tubes cover the entire area of the concrete element and therefore cannot be embedded in concrete. The carbon grid has approximately 69% open surface area allowing the grid to be embedded in the concrete. Light grids are easily formed into a tubular shape and can provide more effective confinement than wraps that are forced to follow the column cross-section, which might be square or rectangular.

This is a new technique that requires investigation of the level of confinement provided by the grids. While there are a number of analytical models available, it is important to conduct testing on concrete samples confined with the light grids to confirm a model that will accurately predict concrete behavior for this specific case.

CONCRETE CONFINEMENT

Confinement can improve both the compressive strength and ductility of concrete. Steel has typically been used to confine the concrete in reinforced concrete columns. Steel can be internal reinforcement, usually used as a spiral, or it can be external such as a steel jacket that is bonded to the outside face of the column. Abdel-Fattah and Ahmad (1989) tested 76 mm x 152 mm concrete cylindrical specimens confined by steel rings spaced at 12.7 mm with the cylinders exhibiting highly ductile behavior. Mei et al (2001) tested 102 mm x 204 mm cylinders with a steel sleeve on the outside. Axial compressive load was applied only to the concrete core. The improvement to the concrete properties was apparent with increased strength and ductility correlating to increases to the thickness of the steel sleeve.

When fiber reinforced polymer (FRP) composites became widely available in the civil sector they started replacing steel as external confinement reinforcement. One of the primary applications of FRP composites is retrofit of concrete elements, primarily columns, to improve their ductility. This is done mainly in seismic regions where concrete structures experience large deformations. Column wrapping improves the strength and ductility of the concrete, which improves the column's performance under earthquake loads.

Xiao and Wu (2000 and 2003), Lam and Teng (2004), Li et al. (2002), Harries and Kharel (2002) and Li and Hadi (2003) tested concrete cylinders wrapped with FRP composites. The strength of FRP confined concrete was increased, compared to the unconfined concrete, between 1% and 420% depending on the type and amount of FRP composite.

Shahawy et al. (2000) tested standard concrete cylinders wrapped with carbon fiber fabrics in an epoxy matrix. The results varied depending on the number of carbon layers applied. For an unconfined concrete strength of 41.4 MPa the confined strength of cylinders was increased to 70 MPa for the 1-layer wrap and 110 MPa for the 4-layer wrap. The ultimate strain for the 1-layer wrap was 0.007 and for the 4-layer wrap 0.016.

Pantelides et al. (1999) wrapped a bridge pier with carbon fiber composites and tested it in situ. An unwrapped pier was also tested. The pier wrapped with carbon was able to accommodate lateral movements two times larger than the unwrapped pier.

Mirmiran et al. (1998) manufactured round and square FRP tubes that were filled with concrete and then tested in compression. The round tubes increased the peak axial stress by as much as 2.5 times the peak axial stress of unconfined concrete and reached axial strains 12 times higher than the axial strain at peak stress of unconfined concrete.

Confinement models to predict the maximum stress or the whole stress-strain curve of confined concrete have been developed (Campione and Miraglia 2003; Li and Hadi 2003; Li et al. 2003; Xiao and Wu 2000, 2003; Fam and Rizkalla 2001). Most models that describe the whole stress-strain curve of FRP confined concrete employ a bilinear curve (second portion of the curve ascending) that in most cases works well. Most models have been refined using data from concrete that is confined by FRP composite materials that their amount and properties produce such behavior. Cases with lower grade material or smaller amounts of FRP composites are scarce and have not been used to demonstrate the applicability of the available models.

CFRP COMPOSITE GRIDS

Heavy CFRP composite grids with thicknesses of half an inch or more are produced and used as primary reinforcement in concrete slabs or bridge decks in an effort to address the problem of corrosion of steel reinforcement due to the use of deicing salts. Rahman et al. (2000) used these carbon grids as reinforcement in a section of concrete deck manufactured in a laboratory. The deck was supported on Steel I beams. They

reported that the behavior of the deck was satisfactory and the carbon grid could replace steel reinforcement in bridge decks. Yost et al. (2001) tested the same type of heavy CFRP grid as reinforcement in concrete beams. The use of the grid as flexural reinforcement, however, resulted in brittle failure due to the rupture of the CFRP grid.

Light carbon grids (thickness 3 to 4 hundredths of an inch) are also available and are used primarily for crack control in concrete structures. Harries and Gassman (2003) conducted tests on reinforced concrete basin knockout panels that employed a light carbon grid to control cracking. The grid reduced cracking of the panel significantly. Shao et al. (2003) used the same light carbon grid to control plastic shrinkage cracking in concrete. They concluded that the plastic shrinkage cracks were reduced by 50% to 65%.

EXPERIMENTAL PROGRAM

Column wrapping with CFRP composites is a popular alternative for improving the seismic resistance of columns. Fiber fabrics and prefabricated FRP composite jackets or tubes cover the entire area of the concrete element and therefore cannot be embedded in concrete. The carbon grid has approximately 69% open surface area allowing the grid to be embedded in the concrete. Light grids are easily formed into a tubular shape and can provide more effective confinement than wraps that are forced to follow the column cross-section, which might be square or rectangular. This is a new technique that requires investigation of the level of confinement provided by the grids. While there are a number of analytical models available, it is important to conduct testing on concrete samples confined with the light grids to confirm a model that will accurately predict concrete behavior for this specific case. Carbon grid properties are essential to any model to determine concrete behavior and need to be determined through testing.

CFRP Grid Testing:

The CFRP composite grid tested in this program was fabricated from carbon fibers embedded in an epoxy matrix. It was supplied in the form of rolls that are 1.041 m wide and 274.32 m long. The strand spacing in the longitudinal direction was 45.7 mm and in the transverse direction 40.6 mm (see Fig. 1). The CFRP grid had an openness of 69% which means that only 31% of the surface area was covered by the carbon fibers.

Tensile properties of the grid were determined by testing two strands from each direction using the specimen configuration shown in Fig. 2(a). Each end of the strand was embedded into a short section of steel pipe for approximately 102 mm. The pipe was then filled with an expansive grout leaving a free length of approximately 202 mm. Two foil strain gauges were placed near the middle of the free-length of the specimen. Steel angles welded to the opposing ends of the pipe anchors were used to attach the specimen to the loading apparatus (Fig. 2(b)). Loading apparatus consisted of a hydraulic actuator mounted to a stiff steel frame in which load was measured with a ring load cell. The average load rate for the 4 specimens was approximately 145 Newtons per second with data acquired approximately every half second.

Table 1 shows the results of the tensile tests. Strands taken from the longitudinal direction are designated longitudinal (L) and strands taken from the transverse direction are designated transverse (T). All the specimens ruptured at peak load. Three specimens ruptured away from the anchor and only one close to the anchor. All specimens ruptured at an interception of a longitudinal and a transverse strand. The average peak load per strand was approximately 4.2 kN and is 16.7% lower than the load provided by the manufacturer (4.9 kN). The average cross sectional area was approximately 6.26 mm². The average strength was approximately 695.5 MPa and the average tensile modulus 64.5 GPa. The strength of each specimen was calculated by dividing the peak load by the cross sectional area while the modulus was determined by a linear regression of the stress-strain data (Fig. 3). The average of the 2 strain gages was used as the strain for each stress level. The data shown in Fig. 3 do not extend to the rupture strength of the specimen because the strain capacity of the strain gauges was exceeded.

Although insufficient tests were conducted to reveal statistical significance, some indication of strength consistency can be determined from the test data. The coefficient of variance (COV) for the strength was 24.2% while for the tensile modulus 17.4%. Both COVs are high and can be attributed to the variability between the CFRP strands. Some strands have a thick layer of epoxy resin covering them, which resulted in a lower fiber volume fraction. According to the manufacturing company (TechFab) strands in both the longitudinal and transverse direction have the same capacity. Our tests indicated a 9% higher capacity for the transverse strands compared to the longitudinal strands but that was attributed to the high variability and the small number of specimens in each direction.

Cylinder Specimens:

Nine standard (152 mm x 304 mm) cylinders were cast. Two layers of grid, formed into concentric tubular configurations and held with plastic ties, were cast into six of the specimens while the remaining three cylinders were cast without reinforcement. The cylinders with the CFRP grid were designated as grid cylinders. The grid cylinders were divided into two groups (3 cylinders in each group) with each group having a different grid diameter. The CFRP grid for the first group was formed into a tubular configuration that was approximately 290-mm long with a diameter of 133.4 mm and a diameter of 139.7 mm for the second grid cylinder group (Fig. 4). Two layers of the grid were applied with the grid lapping the 2 layers for an additional 180 mm for development purposes. The grid openings were aligned to facilitate the flow of concrete through the grid. The CFRP grid round tubes were placed inside plastic cylinder molds and concrete was added (Fig. 5).

A Class II standard FDOT bridge deck concrete mixture was used to make the cylinders. The specified minimum compressive strength of this concrete at 28 days is 31 MPa. Concrete was sampled as per ASTM C172. Both the control and grid cylinders were cast in the field according to ASTM C31 except they were ambient cured rather than moist cured.

996 Michael et al.

All concrete cylinders were allowed to cure in the field inside the plastic mold for approximately one month and were then taken to the laboratory where they remained until 2 weeks before testing. At that time they were removed from their molds and sulfur cement caps were placed on each end. The total curing time for all cylinder specimens was 125 days.

Testing Details:

Nine cylinders (3 control and 6 grid) were tested in displacement control mode in order to capture the post peak behavior of the specimens. Three control cylinders were tested in load control mode using a cylinder tester since no significant post-peak behavior was expected.

The smallest rate that the MTS loading frame could handle was approximately 1.5 mm per minute that resulted in a load rate of approximately 0.73 MPa per second. This load rate is approximately two times higher than the maximum load rate allowed by ASTM C39. Typical load head movement rate and load rate curves from the control cylinders can be seen in Figs 6 and 7 respectively. The same load head movement rate was used for all cylinder specimens tested in displacement control mode.

For the cylinder specimens to be tested in displacement control the 2200 kN loading frame was used. Two Linear Variable Displacement Transducers (LVDTs) were used to continuously record the length change of the specimens as load was applied. The two LVDTs were placed on opposing sides of the cylinder to determine the average length change of the cylinder specimen (Fig. 8). Load and movement data from the loading head as well as data from the LVDTs were collected using a data acquisition program at a rate of 50 Hz. This high rate was necessary to capture the post peak behavior of the cylinders.

Results and Discussion:

The average strength for the control cylinders tested in displacement control mode was 47.8 MPa and the COV 2%. Results from the control cylinders can be found in Table 2. The control cylinders did not exhibit any significant post peak behavior but rather crushed after reaching the peak load. Typical control cylinder types of fracture were: (a) cone and split and (b) cone and shear. A control cylinder after testing can be seen in Fig. 9(a). The stress-strain curves for the control cylinders are depicted in Fig. 10. The first control cylinder after reaching its peak load lost approximately half its strength almost immediately but did not fall apart and continued to carry load contrary to the other two control cylinders that lost all load carrying capacity abruptly soon after peak load.

The average strength of the grid cylinders was 52.9 MPa with a COV of 8.6%. Table 2 contains results from all grid cylinders. Grid cylinders typically failed when CFRP grid strands ruptured. As expected, the concrete cover spalled off of the grid specimens before the peak load was reached but the cylinders maintained most of their load carrying capacity until grid strands started rupturing which took place in sequential rather than in an abrupt manner. The carbon fibers in the CFRP grid are embedded in an epoxy matrix that creates a smooth surface on the outside faces of the CFRP strands, which may have contributed to spalling. A grid cylinder after testing with ruptured hoop CFRP grid

strands can be seen in Fig. 9(b). Experimental stress-axial strain curves for specimens Grid 1 to 3 and specimens Grid 4 to 6 were plotted in Figures 11 and 12 respectively. The stress values for the grid cylinders were calculated based on the area of the concrete core enclosed by the CFRP grid and the axial strain was calculated as the average change in the length, measured by the 2 LVDTs, of the cylinder over the original length.

The post peak behavior for all grid cylinders was different than that of control cylinders. Grid cylinders reached higher peak loads and accommodated larger displacements than the control cylinders. This is especially evident in Fig. 13 where typical experimental stress-axial strain curves from both control and grid specimens were plotted. The area under the post peak curve of the grid cylinders was approximately 3 times larger than the area of the control cylinders. Specimens Grid 4, 5 and 6 had approximately 15% more area under the stress-strain curve than specimens Grid 1 and 3. Specimen Grid 2 had approximately 45% more area under the curve than Grid 1 and 3 and 25% more area than specimens Grid 4, 5 and 6.

All grid cylinders reached a peak axial load followed by a descending post peak curve. Other researchers observed such a behavior in lightly confined concrete. Harries and Kharel (2003) made similar observations for their one and two-ply E-Glass confined cylinders. Sfer et al. (2002) studied the behavior of concrete under triaxial compression and their axial stress-strain curves at low confining pressures had a descending post peak curve. The increase in the concrete strength was between 10% and 20%, which compares to the 11% increase observed for our cylinders. In the case of the CFRP grid confined concrete even with the two layers the concrete is still considered lightly confined since the two CFRP grid layers add up to less than 1 layer of carbon fiber fabric when the CFRP grid strand thickness is spread uniformly over the surface area of the concrete core. In addition the strength and modulus of the CFRP grid was found to be lower than typical carbon composites, which further reduces its confinement effectiveness. Therefore, the post peak behavior observed for the CFRP grid cylinders verifies the observations made by Harries and Kharel (2003) and Sfer et al. (2002).

CONFINEMENT MODEL

The present study is a part of a related project in which an all carbon reinforced concrete pile is being evaluated for use in Florida's highly corrosive coastal environment. CFRP grid is one of the materials being evaluated as potential reinforcement. It is anticipated that the piles will be designed to behave, when loaded in flexure, in an over-reinforced manner to avoid the brittle failure mode that is usually precipitated by rupture of the FRP reinforcement. One aspect of the pile design is that the confinement provided by the grid will improve the flexural ductility of the compression zone, perhaps providing a more favorable failure mode than the rupture of the FRP flexural reinforcement.

Most models for concrete confined with CFRP reinforcement are based on the fact that, in most cases, a single layer of carbon fabric will provide adequate reinforcement to sufficiently confine the concrete. When the CFRP grid is used as confinement reinforcement it is expected that the confining pressure and confinement effectiveness

998 Michael et al.

would be less than that of a fully jacketed system. Therefore models developed using data from relatively highly confined concrete may not be adequate.

Several existing models were investigated to model the behavior of CFRP grid confined concrete. All of the existing models examined are based on a constant thickness of the FRP material that fully covers the external surface of the concrete. The hoop grid strands only cover part of the area. One approach when using the existing models is to determine an equivalent full coverage thickness for the hoop strands. The equivalent grid thickness (t_{eg}) was calculated based on the following expression:

$$t_{eg} = \frac{n_l \cdot n_{gs} \cdot b_g \cdot t_g}{h} \quad (1)$$

where: n_l is the number of CFRP grid layers, n_{gs} is the number of grid strands, b_g is the width of the grid strands, t_g is the thickness of the grid strands and h is the height of the cylinder. For columns or other concrete elements that have large axial lengths Eq. 1 can be simplified as follows:

$$t_{eg} = \frac{n_l \cdot b_g \cdot t_g}{s_g} \quad (2)$$

where: s_g is the CFRP grid strand spacing.

The secant modulus of elasticity of concrete (E_c) was calculated based on existing empirical expressions (Nawy 2003):

$$E_c = 4730 \cdot \sqrt{f'_c} \quad (3)$$

where: f'_c is the minimum specified compressive strength of concrete, in N/mm^2 , at 28 days.

To determine the confinement strength (f_{ru}) simple pressure vessel mechanics were used. The equilibrium condition requires the force from the confining strength be equal to the force in the FRP encasement. The force from confinement is equal to the confining strength times the diameter of the enclosed concrete and the force in the encasement is equal to the strength of the encasement times twice the thickness of the FRP encasement. By rearranging the equation the confinement strength (f_{ru}) was found:

$$f_{ru} = \frac{2 \cdot t_{eg}}{d_g} \cdot f_{gu} \quad (4)$$

where f_{ru} is the confinement strength, d_g is the diameter of the CFRP grid tube and f_{gu} is the ultimate strength of the CFRP grid strands.

Assuming that the confined concrete is in a triaxial stress state, the increase in strength provided by the confinement is reflected in the maximum stress (f''_{cc}) for a cylindrical specimen, which is defined as (Mander et al.1988):

$$f''_{cc} = f'_c + k_1 \cdot f_{ru} \quad (5)$$

where k_1 is the confinement effectiveness coefficient. The confinement effectiveness coefficient for concrete confined by steel is usually taken between 2.8 and 4.1. Campione and Miraglia (2003) found that the above values overestimate the confinement effectiveness coefficient for concrete wrapped with FRP. They found the confinement effectiveness coefficient for FRP wrapped concrete to be 2. For the purpose of this study the confinement effectiveness coefficient was taken as 2.

The axial strain of CFRP grid confined concrete at the peak stress (ε_{co}) was determined in a similar manner as unconfined concrete using the following expression (MacGregor 1997):

$$\varepsilon_{co} = 1.8 \cdot \frac{f''_{cc}}{E_c} \quad (6)$$

Equations (5) and (6) were combined with the modified Hognestad stress-strain equation as follows:

$$f_c = f''_{cc} \cdot \left[\frac{2 \cdot \varepsilon_c}{\varepsilon_{co}} - \left(\frac{\varepsilon_c}{\varepsilon_{co}} \right)^2 \right] \quad (7)$$

$$f_c = f''_{cc} \cdot [1 - D_c \cdot (\varepsilon_c - \varepsilon_{co})] \quad (8)$$

where ε_c is the concrete strain, ε_o is the strain at peak stress of unconfined concrete and ε_{cu} is the ultimate strain. These equations are plotted in Fig. 14. The modified Hognestad equations model the ascending branch (AB) with a parabolic relationship and the descending branch BC with a linearly descending curve. The equation for region BC is based on the deterioration constant (D_c) that controls the slope of the line.

The material properties of the CFRP grid strands were used to construct the stress-strain curve of the CFRP grid confined concrete. The average strength of the control cylinders tested in displacement control mode was taken as the strength of unconfined concrete (f'_c). An average CFRP grid tube diameter of 136.5 mm was used. The ultimate concrete strain ε_{cu} was assumed to be 0.00725 mm/mm. The average stress-strain curve for the CFRP grid confined concrete was constructed using data from all grid cylinders. The average stress-strain curve for the control cylinders was also constructed for comparison. The deterioration constant was taken equal to 120 to match post peak experimental data. All three curves are depicted in Fig. 15. The modified Hognestad matches well with the experimental curve. The average experimental peak stress was 52.9 MPa while the model predicted a peak stress of 52 MPa. The predicted value is 1.7%

1000 Michael et al.

lower than the experimental average. The average experimental strain at the peak stress was 0.00259 mm/mm while the model predicted a strain of 0.00288 mm/mm at peak stress. The predicted strain value is 11.2% higher than the average experimental value.

CONCLUSIONS

Concrete cylinders with embedded tubular CFRP grids were tested in compression to failure to determine the post-peak behavior and ability of the grid to provide confinement to the concrete. It was found that the CFRP grid does not produce a highly confined concrete. This was expected since the amount of CFRP material provided by the grid is low due to its large openings. Significant improvement, however, was observed in the ductility of the concrete cylinders with embedded CFRP grid. Grid confinement also resulted in an increase in the concrete strength of approximately 10.7%. The larger CFRP grid diameter cylinders were more ductile compared to the smaller CFRP grid diameter cylinders with the exception of cylinder Grid 2. However the difference in diameters and the number of cylinders are small and therefore this conclusion is drawn with caution.

The equivalent grid thickness is a valid way of converting the concentrated thickness of the CFRP grid to an equivalent thickness over the surface area of the concrete core. Model results demonstrate that. The modified Hognestad provides an accurate prediction of the behavior of concrete confined with the CFRP grid.

ACKNOWLEDGMENTS

This study is sponsored by the Florida Department of Transportation. The authors gratefully acknowledge the contributions of Steve Eudy who set up and ran the data acquisition system, as well as Frank Cobb, Tony Johnston, Paul Tighe, and David Allen who helped prepare the testing apparatus.

NOTATION

t_{eg}	=	equivalent grid thickness
n_l	=	number of grid layers
n_{gs}	=	number of grid strands
b_g	=	width of grid strands
t_g	=	thickness of grid strands
h	=	height of cylinder
s_g	=	spacing of grid strands
E_c	=	secant modulus of elasticity of concrete
f'_c	=	unconfined concrete strength
f_{ru}	=	confinement strength
d_g	=	diameter of grid tube
f_{gu}	=	ultimate strength of grid strands
f_{cc}	=	confined concrete strength
k_1	=	confinement effectiveness coefficient
ϵ_{co}	=	concrete axial strain at peak stress

f_c	=	concrete stress
ε_c	=	concrete axial strain
D_c	=	deterioration constant
ε_{cu}	=	ultimate concrete axial strain

REFERENCES

Referenced Standards

ASTM

- C 31 Standard Practice for Making and Curing Concrete Test Specimens in the Field
- C172 Standard Practice for Sampling Freshly Mixed Concrete
- C 39 Standard Test Method for Compressive Strength of Cylindrical Concrete Specimens

These publications may be obtained from this organization:

ASTM International
 100 Barr Harbor Drive
 West Conshohocken, PA 19428

Cited References

- Abdel-Fattah, H. and Ahmad, S. H., (1989), "Behavior of Hoop-Confined High-Strength Concrete under Axial and Shear Loads", *ACI Structural Journal*, Vol. 86, No 6, pp. 652-659.
- Campione, G., Miraglia, N., (2003), "Strength and Strain Capacities of Concrete Compression Members Reinforced with FRP", *Cement and Concrete Composites*, Vol. 25, No 1, pp. 31-41.
- Fam, A. Z. and Rizkalla, S. H., (2001), "Confinement Model for Axially Loaded Concrete Confined by Circular Fiber-Reinforced Polymer Tubes", *ACI Structural Journal*, Vol. 98, No 4, pp. 451-461.
- Harries, K. A. and Gassman, S. L., (2003), "Load Tests of Reinforced Concrete Catch Basing Knockout Panels", *Department of Civil and Environmental Engineering, University of South Carolina*, Report No ST03-01, p. 21.
- Harries, K. A., and Kharel, G., (2002), "Experimental Investigation of the Behavior of Variably Confined Concrete", *Cement and Concrete Research*, Vol. 33, No 6, pp. 873-880.
- Lam, L., and Teng, J. G., (2004), "Ultimate Condition of Fiber Reinforced Polymer-Confined Concrete", *Journal of Composites for Construction*, Vol. 8, No 6, pp. 539-548.
- Li, J., Hadi, M.N.S., (2003), "Behaviour of Externally Confined High-Strength Concrete Columns Under Eccentric Loading", *Composite Structures*, Vol. 62, No 2, pp. 145-153.
- Li, Y., Lin, C. and Sung, Y., (2002), "Compressive Behavior of Concrete Confined by Various Types of FRP Composite Jackets", *Mechanics of Materials*, Vol. 35, No 3-6, pp. 603-619.

1002 Michael et al.

MacGregor, J. G., (1997), "Chapter 3: Materials", *Reinforced Concrete: Mechanics and Design*, Third Edition, Prentice Hall, New Jersey, pp. 35-81.

Mander, J. B., Priestley, M. J. N. and Park, R., (1988), "Theoretical Stress-Strain Model for Confined Concrete", *Journal of Structural Engineering*, Vol. 114, No 8, pp. 1804-1826.

Mei, H., Kiousis, P. D., Ehsani, M. R. and Saadatmanesh, H., (2001), "Confinement Effects on High-Strength Concrete", *ACI Structural Journal*, Vol. 98, No 4, pp. 548-553.

Mirmiran, A., Shahawy, M., Samaan, M., El Echary, H., Mastrapa, J. C. and Pico, O., (1998), "Effect of Column Parameters on FRP-Confined Concrete", *Journal of Composites for Construction*, Vol. 2, No 4, pp. 175-185.

Nawy, E. G., (2003), "Chapter 3: Concrete", *Reinforced Concrete: A Fundamental Approach*, Fifth Edition, Prentice Hall, New Jersey, pp. 20-67.

Pantelides, C. P., Gergely, J., Reaveley, L. D. and Volnyy, V. A., (1999), "Retrofit of RC Bridge Pier with CFRP Advanced Composites", *Journal of Structural Engineering*, Vol. 125, No 10, pp. 1094-1099.

Park, R. and Paulay, T., (1975), "Chapter 6: Ultimate Deformation and Ductility of Members with Flexure", *Reinforced Concrete Structures*, John Wiley & Sons, New York, pp. 195-269.

Rahman, A. H., Kingsley, C. Y. and Kobayashi, K., (2000), "Service and Ultimate Load Behavior of Bridge Deck Reinforced with Carbon FRP Grid", *Journal of Composites for Construction*, Vol. 4, No 1, pp. 16-23.

Sfer, D., Carol, I., Gettu, R. and Etse, G., (2002), "Study of the Behavior of Concrete under Triaxial Compression", *Journal of Engineering Mechanics*, Vol. 128, No 2, pp. 156-163.

Shahawy, M., Mirmiran, A. and Beitelman, T., (2000), "Tests and Modeling of Carbon-Wrapped Concrete Columns", *Composites Part B: Engineering*, Vol. 31, No 6-7, pp. 471-480.

Shao, Y., Johnson, C. and Mirmiran, A., (2003), "Control of Plastic Shrinkage Cracking of Concrete with TechFab Carbon FRP Grids", *Department of Civil, Construction, and Environmental Engineering, North Carolina State University*, Report to Tech-Fab Inc, p. 7.

Xiao, Y. and Wu, H., (2000), "Compressive Behavior of Concrete Confined by Carbon Fiber Composite Jackets", *Journal of Materials in Civil Engineering*, Vol. 12, No 2, pp. 139-146.

Xiao, Y. and Wu, H., (2003), "A Constitutive Model for Concrete Confinement with Carbon Fiber Reinforced Plastics", *Journal of Reinforced Plastics and composites*, Vol. 22, No 13, pp. 1187-1201.

Yost, J. R., Goodspeed, C. H. and Schmeckpeper, E. R., (2001), "Flexural Performance of Concrete Beams Reinforced with FRP Grids", *Journal of Composites for Construction*, Vol. 5, No 1, pp. 18-25.

Table 1 – Results for CFRP Grid Specimens

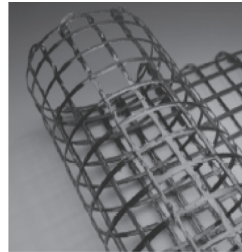
Specimen	Grid Roll Direction	Area (mm ²)	Peak Load (kN)	Strength (MPa)	Modulus (GPa)
T1	Transverse	7.91	3.74	472.5	52.9
T2	Transverse	5.86	5.10	870.2	58.9
L1	Longitudinal	6.08	4.11	675.5	66.7
L2	Longitudinal	5.18	3.96	763.8	79.4

Table 2 – Results of Grid Cylinders Tested in Displacement Control Mode

Type	Grid Diam. (mm)	Peak Load (kN)	Strain at Peak Load (mm/mm)	Conc. Core Area (mm ²)	Peak Stress (MPa)	Aver. Stress (MPa)	COV (%)
Control 1	N/A	854.8	0.00251	18241	46.9	47.8	2
Control 2	N/A	853.2	0.00232	18241	48.8		
Control 3	N/A	870.6	0.00236	18241	47.7		
Grid 1	133.4	820.8	0.00281	13966	58.8	52.9	8.6
Grid 2	133.4	650.7	0.00200	13966	46.6		
Grid 3	133.4	792.6	0.00256	13966	56.8		
Grid 4	139.7	743.5	0.00279	15328	49.6		
Grid 5	139.7	775.9	0.00256	15328	51.8		
Grid 6	139.7	803.7	0.00279	15328	53.7		



(a)



(b)

Figure 1 – (a) CFRP Grid Rolls and (b) CFRP Grid Formed into a Tubular Configuration Necessary to Confine Concrete. (Photos Courtesy of TechFab)

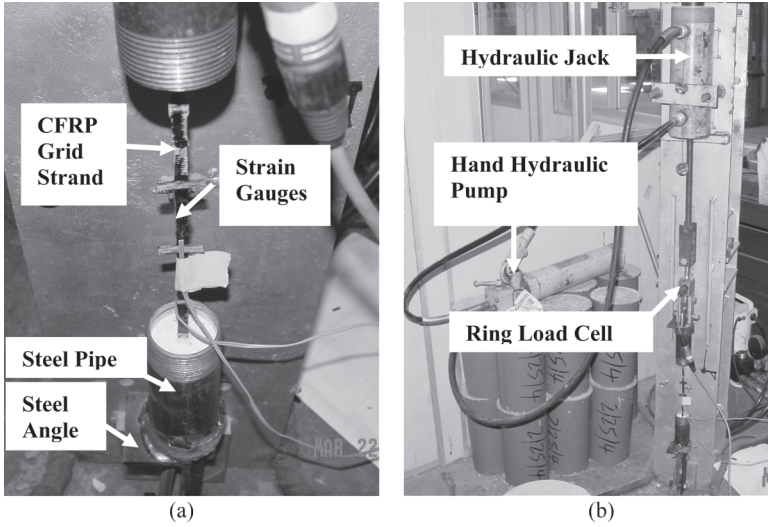


Figure 2 – (a) CFRP Grid Stand Specimen and (b) Test Set-Up for Tensile Testing of CFRP Grid Strands

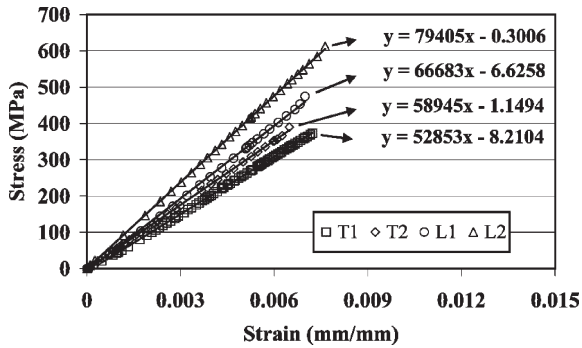


Figure 3 – Stress-Strain Curves of CFRP Grid Tensile Tests

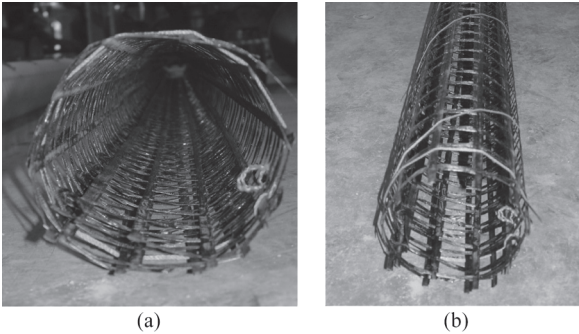


Figure 4 - CFRP Grid Round Tubes: (a) Cross Sectional View and (b) Longitudinal View



Figure 5 – CFRP Grid Cylinder Casting in the Field: (a) Beginning of Cylinder Casting and (b) Finishing Cylinder Casting

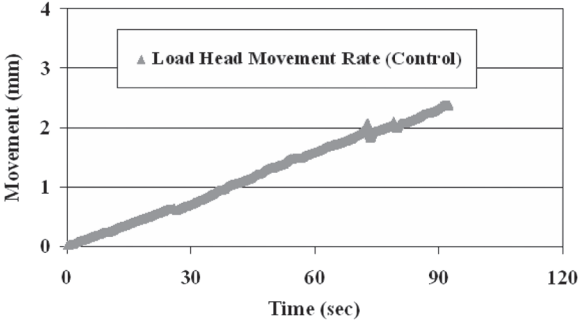


Figure 6 – Typical Load Head Movement Rate for Control Cylinders

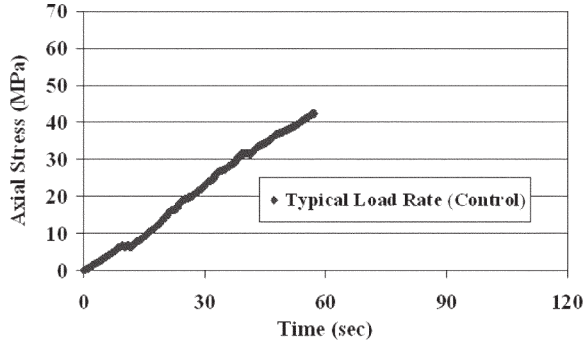


Figure 7 – Typical Load Rate for Control Cylinders

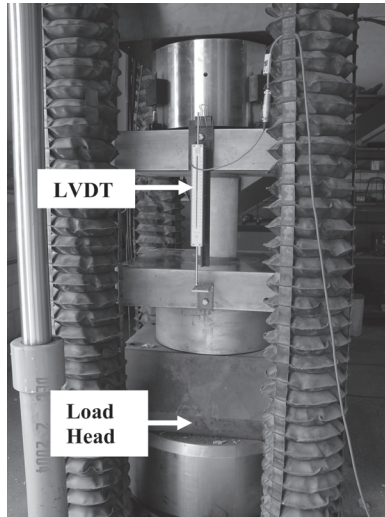


Figure 8 – CFRP Grid Cylinder Test Set-Up

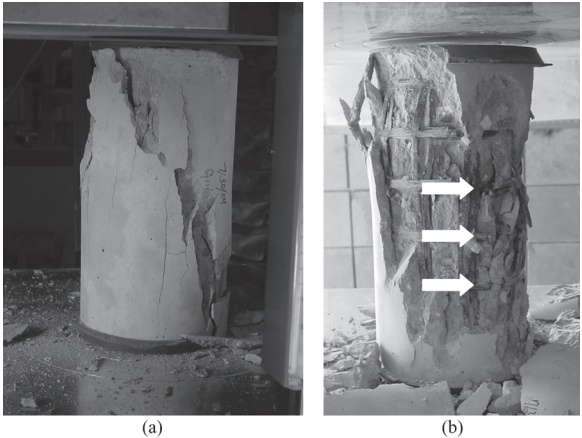


Figure 9 – Cylinders after Testing: (a) Control Cylinder, and (b) Grid Cylinder (Arrows Indicate Ruptured CFRP Grid Strands)

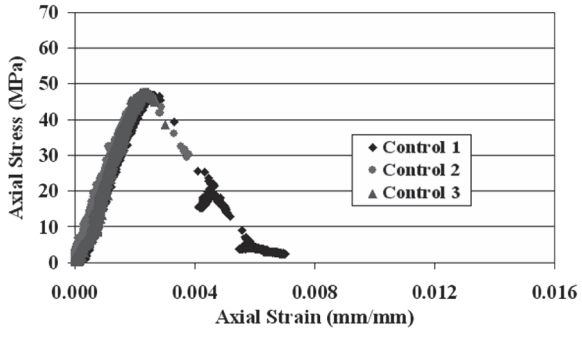


Figure 10 – Stress-Strain Curves for Control Cylinders

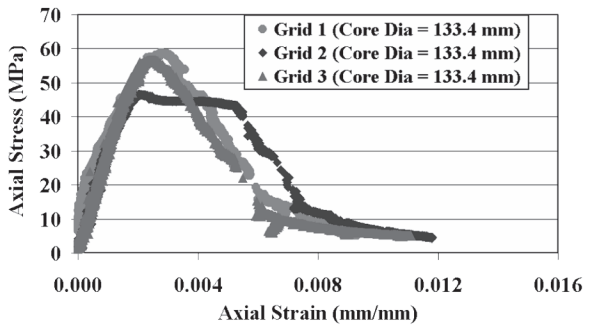


Figure 11 - Stress-Strain Curves for the 133.4 mm Core Diameter Grid Cylinders

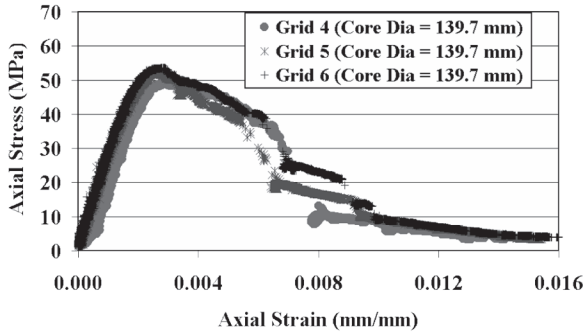


Figure 12 - Stress-Strain Curves for the 139.7 mm Core Diameter Grid Cylinders

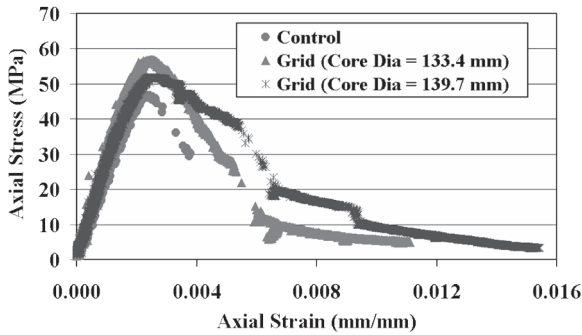


Figure 13 – Stress-Strain Curves for Typical Control and Grid Cylinders

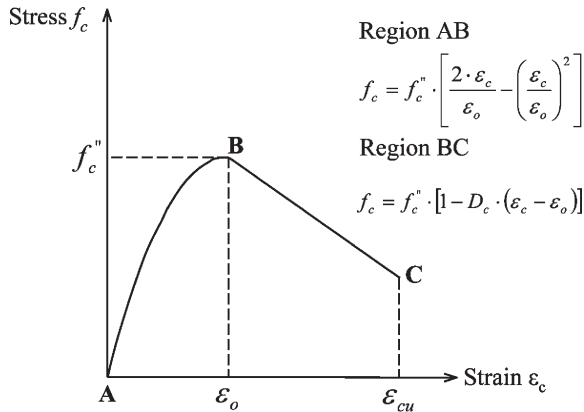


Figure 14 – Modified Hognestad Stress Strain-Curve (Taken from Park and Pauly 1975)

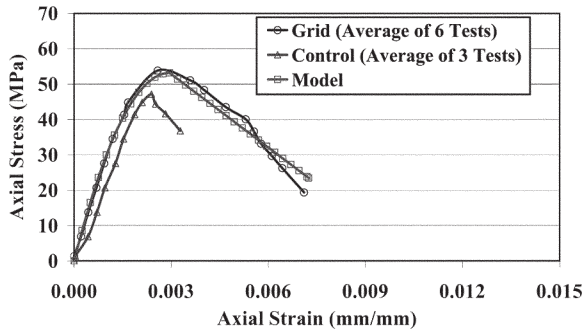


Figure 15 – Average Experimental Stress-Strain Curves of Control and Grid Cylinders and the Modified Hognestad Model for CFRP Grid Confined Concrete

